CORPUS PUBLISHERS

Journal of Mineral and Material Science (JMMS)

ISSN: 2833-3616

Volume 5, Issue 4, 2024

Article Information

Received date : July 26, 2024

Published date: September 16, 2024

*Corresponding author

Freddy Humberto Escobar, Universidad Surcolombiana, Neiva, Colombia

Keywords: Hydraulic Fracturing; Pressure Transient Analysis; Fracture Interconnexion; FracHits; Shale Reservoirs

DOI: 10.54026/JMMS/1092

Research Article

Estimating Fracture Interconnection in Shale Reservoirs Using the TDS Technique: A Three-Well Model Analysis

Freddy Humberto Escobar[1]*, David Fernando Gómez Gil[2] and Jalal F Owayed[3]

[1]*Universidad Surcolombiana, Neiva, Colombia*

[2]*Sierracol Energy, Bogotá, Colombia*

[3]*Kuwait University, Safat, Kwait*

Abstract

In shale reservoirs, efficient hydrocarbon extraction relies on the Stimulated Reservoir Volume (SRV) created by hydraulic fracturing. This study develops and applies direct analytical equations to determine the degree of fracture interconnection in a three-horizontal-well system using transient pressure and flow rate analysis with the TDS technique. The equations estimate permeability, area, and the epsilon (ε) parameter, representing the fracture interconnection fraction. They are applied to both pressure drawdown and buildup tests, as well as transient rate analysis in oil and gas wells. These equations were successfully verified using synthetic data, demonstrating their accuracy and usefulness. The methodology effectively identifies fracture interconnections and their impact on well productivity. This approach enables practical mitigation strategies to prevent rapid depletion of new wells.

Nomenclature: A: Drainage area, ft^2; B: Oil volume factor, rb/STB; c_t: Total compressibility, 1/psi; f_{corr}: Correction factor; h: Formation thickness, ft; k: SRV Permeability of the Observation Well, md; L_w: Horizontal well length, ft; m(P): Pseudopressure function, psi^2/cp; P: Pressure, psi; P_D: Dimensionless pressure; P_i: Initial pressure, psi; P_{wf}: Well-flowing pressure, psi; q: Oil flow rate, BPD; q_g: Gas flow rate, MSCF/D; 1/q: Reciprocal rate, 1/BPD (oil) or Day/Mscf (gas); r_w: Wellbore radius, ft; t: Time, hrs; t*ΔP': Pressure derivative, psi; t*Δm(P)': Pseudopressure derivative, psi^2/cp; t*(1/q'): Reciprocal rate derivative, 1/BPD (oil) or Day/Mscf (gas); t_D: Dimensionless time referred to half-fracture length; t_D*P_D': Dimensionless pressure derivative; $t_D*m(P_D')$: Dimensionless pseudopressure derivative; $t_D*(1/q_D')$: Dimensionless reciprocal rate derivative; T: Reservoir temperature, °R; X_D: Dimensionless distance in the x-direction; X_{eA}: Reservoir half-length at well A, md; X_f: Half-fracture length, md

Subscripts: 1l: first linear flow regime; 1lpssi: Intercept of the straight lines between the first linear flow regime and the pseudosteady-state period; A,B,C: Wells; corr: Correction; D: Dimensionless quantity; g: Gas; i: Initial conditions, intercept; maxd1l: Maximum point of the dimensionless pressure derivative in the downward concavity after the first linear flow regime; mind1l: Minimum point of the dimensionless pressure derivative in the upward concavity after the first linear flow regime; o: Oil; p1qq': Late time of interception of the reciprocal rate and reciprocal rate derivative; pss: Pseudosteady-state; pss-int: Intercept of the dimensionless pressure derivative line; wf: At well-flowing pressure

Greek: Δ: Change, drop; ε: Parameter indicating the degree of connectivity between the neighboring wells B and C with the observation well, well A. (Positive epsilon indicates there is an influx into well A); ϕ: Porosity, fraction; μ: Viscosity, cp

Introduction

One of the major challenges for oil companies is to maximize resource utilization in a given area, especially in shale reservoirs. In these cases, only the hydrocarbon present in the hydraulically fractured zone, known as SRV (Stimulated Reservoir Volume), can be extracted. This is mainly due to the low permeability values of shale formations, making the optimization of spacing between horizontal multi-fractured wells (HWMF) a viable solution to increase recovery. In the extraction of hydrocarbons from shale reservoirs, only the area that is fractured can be drained, resulting in a SRV. For this reason, it is necessary to drill multiple horizontal multi-fractured wells (HWMF) to extract the fluids from the reservoir. When drilling development HWMFs near wells that have already been producing for a long period, it is common for the fractures of the new wells to connect with the fractures of the existing wells, a phenomenon known as "Frac-Hits" or fracture interconnection. The more fractures that interconnect between wells, the lower the productivity of the new wells, because the connection of fractures with already produced wells creates a pressure equilibrium in the reservoir, resulting in a rapid depletion of the new well.However, drilling wells near others that are already depleted can temporarily or permanently reduce the productivity of the new well and affect the performance of nearby wells. The region around wells close to the development well, affected by a pressure decrease due to previous extraction, acts as a low-pressure area. This facilitates the interconnection of hydraulic fractures generated in the new wells with those of existing wells. This phenomenon, known as Fracture-Driven Interactions (FDI) or "Frac Hits", Jacobs [1], is referred to as fracture interconnection in this article. Fracture interconnections result from the propagation of new hydraulic fractures generated in the development wells towards existing fractures in the formation, Lawal et al. [2]. This interaction can occur through primary fractures, originated by hydraulic fracturing, or secondary fractures, which are part of the natural or induced fracture network in the formation, Jia et al. [3,4]. Figure 1 shows a clear example of the fracture interconnection that can occur between HWMFs.

Figure 1: Three-well system HMFW (A, B, C), Taken from: (Hetrick LH [5]).

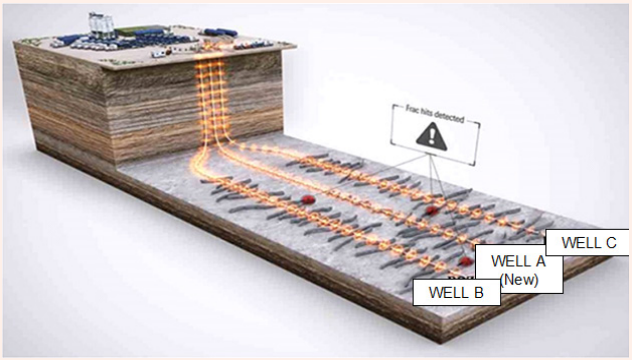

In Figure 1, it can be observed how some of the fractures from Well A (new well) interconnect with the fractures from Wells B and C. To understand why this phenomenon occurs, we must assume that Wells B and C were drilled at least 12 months before Well A, and therefore, have already had production time. Due to the presence of an undrained area between Wells B and C, it was decided to drill a HMWF well, called Well A, between these existing wells, which have lost pressure due to their productivity in recent months. This allows the hydraulic fractures from Well A to easily connect with the low-pressure zones around the depleted wells, thereby increasing the risk of fracture interconnection, integrity issues in the wells, and even blowouts in the main wells [6]. The more fractures from the new well that interconnect with nearby wells, the lower the productivity of the development well. The literature presents several fracture interconnection models, including the physical model by Yu et al. [7] and the mathematical models by Molina & Zeodouni [8-10]. The TDS methodology was introduced by Tiab [11] for the rapid, effective, and accurate interpretation of pressure tests and pressure derivatives using characteristic points obtained from the derivative graph. This technique was also extended to transient flow tests. Some examples of TDS technique applications to shale reservoirs were presented by Bernal, et al. [12-15]. Additionally, Escobar, et al. [16] presented an extension of the TDS technique in interference tests on horizontal wells connected by an extensive hydraulic fracture.

Due to the impacts that fracture interconnections have on oil companies, several methods have been proposed to detect and evaluate the impact of these interconnections on well performance and EUR (Estimated Ultimate Recovery). Gomez-Gil & Sacananby [17] used the mathematical model proposed by Molina [10] to interpret pressure and transient flow tests using the TDS technique. In this work, based on the Gomez-Gil & Sacanambuy [17] work, mathematical expressions were generated to determine the permeability (k), area (a), and epsilon (ε) parameters of the observation well from the interpretation of transient pressure and rate transient tests using the TDS technique. A methodology is also presented to identify the fraction of interconnected fractures through transient pressure and flow rate analysis. A mathematical model using the epsilon (ε) parameter, representing the fraction of interconnected fractures between two nearby wells and an observation well, is employed. The value of ε can range from -1 to 1, where 0 indicates no fracture interconnection. When $0 < \varepsilon < 1$, it indicates the fraction of fractures interconnected with nearby wells and the dominant flow direction is from the nearby wells to the observation well. When $-1 < \varepsilon < 0$, it also indicates the fraction of interconnected fractures, but in this case, the dominant flow direction is from the observation well to the neighboring wells.

It was identified that when $\varepsilon \neq 0$, it is necessary to adjust the area calculation determined from the interpretation of the transient pressure or flow rate test, due to the deviation in the SRV area estimation of the observation well, which can be underestimated or overestimated. This deviation is due to the pressure response from the nearby wells to the observation well and is directly related to the degree of fracture interconnection between the wells. To adjust the SRV area calculation of the observation well, a correction factor related to the value of ε calculated from the test interpretation was estimated. The use of the equations generated in this work allows for a practical, rapid, and reliable estimation of the fraction of interconnected fractures between HWMFs. By estimating this fraction, mitigation actions can be established to prevent the rapid depletion of new wells.

Formulation and Transient Behavior

The mathematical model proposed by Molina [10] was used to generate both pressure and pressure derivative curves as well as reciprocal flow rate and reciprocal flow rate derivative curves for different permeability conditions (k), degrees of fracture interconnection between nearby wells and the observation well (ε), as well as varying the fracture length (xf), which is directly related to the SRV area. However, in this work the permeability in the tree wells is assumed that are about the same which is a good guess since the wells are nearby. The dimensionless time, dimensionless pressure and dimensionless pressure derivative for oil reservoir are given by, respectively,

The dimensionless time, dimensionless pseudopressure and dimensionless pseudopressure derivative for gas reservoir are given by, respectively,

$$t_D = \frac{0.0002637 k_o t}{\phi \mu c_t x_f^2} \quad (1)$$

$$P_D = \frac{k_o h \Delta P}{141.2 q u B} \quad (2)$$

$$t_D * P_D' = \frac{k_o h (t * \Delta P')}{141.2 q \mu B} \quad (3)$$

The dimensionless reciprocal rate and dimensionless reciprocal rate derivative for gas reservoir are given by, respectively,

$$t_D = \frac{0.0002637 k_g t}{\phi (\mu c_t)_i x_f^2} \quad (4)$$

$$m(P)_D = \frac{k_g h [\Delta m(P)]}{1422.52 q_{sc} T} \quad (5)$$

$$t_D * m(P)'_D = \frac{k_g h [t * \Delta m(P)']}{1422.52 q_{sc} T} \quad (6)$$

The dimensionless reciprocal rate and dimensionless reciprocal rate derivative for oil reservoir are given by, respectively,

$$\frac{1}{q_D} = \frac{k_o h (P_i - P_{wf})}{141.2 \mu B} (1/q) \quad (7)$$

$$t_D * (1/q_D)' = \frac{k_o h (P_i - P_{wf})}{141.2 \mu B} [t * (1/q_o)'] \quad (8)$$

The dimensionless reciprocal rate and dimensionless reciprocal rate derivative for gas reservoir are given by, respectively,

$$1/q_D = \frac{k_g h [\Delta m(P)]}{1422.52 T} (1/q_g) \quad (9)$$

$$t_D * (1/q_D)' = \frac{k_g h [\Delta m(P)]}{1422.52 T} [t * (1/q)_g'] \quad (10)$$

From the simulation results, points or slopes were identified that allow the determination of parameters such as k, ε, and area. For the development of each proposed equation, a series of simulations was generated where the variable of interest was modified while the other variables remained constant. Subsequently, the data were graphed, and an adjustment was made to find a unique behavior in the graphs. The pressure derivative behavior is shown in Figure 2. The following flow regimes and characteristics can be observed: Linear Flow Regime: In this flow, the first pressure response of the well is observed, showing the flow through the fractures of the SRV zone.

Figure 2: Characteristic flow regimes of the pressure derivative vs. time in dimensionless form.

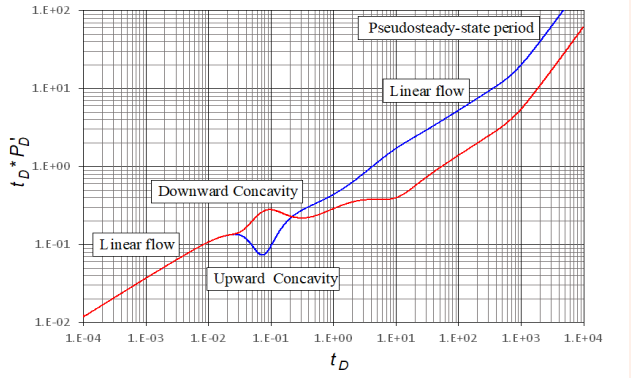

After unifying the linear flow regime period, the following expression was obtained:

$$(t_D * P_D') * k_o = 10.43(t_D)^{0.5} \quad (11)$$

By substituting Equations (1) and (3) into Equation (12) and solving for oil permeability, the following result is obtained:

$$k_o = 8.297\left(\frac{qB}{h(t*\Delta P')_{1l}}\sqrt{\frac{\mu t_{1l}}{\phi c_t x_f^2}}\right)^{0.6666} \quad (12)$$

Since Equation (11) is also applied to the dimensionless pseudopressure derivative, substituting Equations (4) and (6) into Equation (11) and solving for gas permeability yields:

$$k_g = 11.210\left(\frac{B}{h(\Delta P)(t*1/q')_{1l}}\sqrt{\frac{\mu t_{1l}}{\phi c_t x_f^2}}\right)^{0.6452} \quad (13)$$

Flow Regime with Upward or Downward Concavity: It was observed that by varying ε from -1 to 1, an upward or downward concavity is formed, indicating the degree of connectivity of the observation well with the nearby wells. Downward Concavity: In this regime, the interconnection of fractures from the observation well A with nearby wells B and C is evidenced. When a downward concavity is observed after the first linear flow, it indicates an influx from the neighboring wells into the observation well.

Figure 3 shows the pressure derivative behavior for different negative ε values. When plotting the dimensionless pressure derivative divided by ε0.18 for different ε values (Figure 4), a unified maximum point is found after the first linear flow regime.

The governing equation for this behavior is given by:

$$\frac{t_D * P_D'}{\varepsilon^{0.18}} = 0.278 \quad (14)$$

Figure 3: Pressure derivative vs. time for different negative values of epsilon (ε).

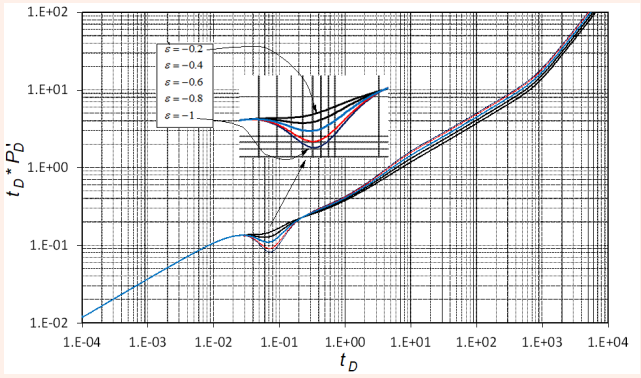

Figure 4: Graph of unique behavior in the minimum value of the upward concavity.

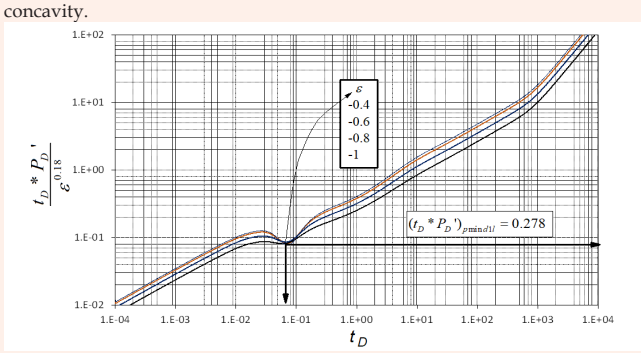

By substituting the dimensionless quantities given by Equations (3) and (6) into Equation (14) and solving for positive ε, we obtain the following for both oil and gas wells, respectively:

$$\varepsilon = \sqrt[0.18]{\left(\frac{k_o h(t*\Delta P')_{p\max dl}}{39.2012 q\mu B}\right)} \quad (15)$$

$$\varepsilon = \left(\frac{57.89\mu B}{k_g h(\Delta P)(t*1/q')_{p\min dl}}\right)^{-2.31} \quad (16)$$

Upward Concavity: In this regime, the interconnection of fractures from the observation well A with nearby wells B and C is also evidenced. When an upward concavity is observed after the first linear flow, it indicates a flow from the observation well to the neighboring wells. Similarly, when plotting the dimensionless pressure derivative multiplied by ε0.48 for different ε values, a unified behavior during the concavity is found. The governing equation for this minimum point is:

$$(t_D * P_D')\varepsilon^{0.48} = 0.0826 \quad (17)$$

Once again, by substituting Equations (3) for oil wells and (6) for gas wells into Equation (17) and solving for negative ε, we obtain the following for both oil and gas wells, respectively:

$$-\varepsilon = (155.357)^{-0.48}\sqrt{\frac{k_o h(t*\Delta P')_{p\min dl}}{q\mu B}} \quad (18)$$

$$-\varepsilon = 30.621\left(\frac{\mu B}{k_g h(\Delta P)(t*1/q')_{p\min dl}}\right)^{0.6452} \quad (19)$$

Second Linear Flow Regime: In this flow regime, the pressure response of the flow from the SRV zone of wells B and C to well A is observed. Pseudo-Steady State Flow Regime: This regime manifests the pressure response reaching the boundaries of the SRV area. If there is fracture interconnection, a pressure response from the nearby wells B and C is also obtained. Figure 5 displays the pressure behavior for different reservoir areas.

Figure 5: Pressure derivative vs. time log-log plot for different reservoir areas ($A=X_{eA}*X_f$, $X_f=100$)

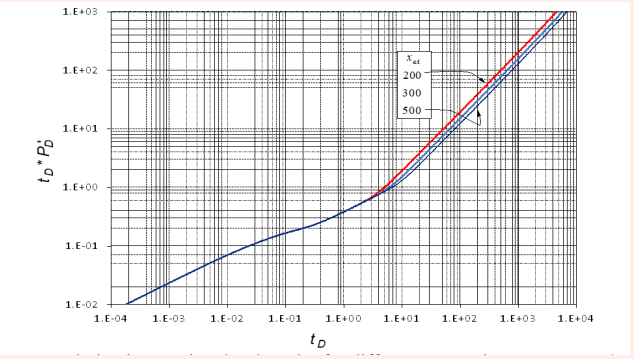

As observed, the late pseudosteady-state period has a unique slope of one but different intercepts. A unified pseudo-steady-state line is presented in Figure 6, with the governing equation provided below:

$$(t_D * P_D')_{pss}(x_{eAi}x_f)^{0.85}2n_f = 674095.2525(t_D)_{pss}$$

Figure 6: Graph of unique behavior during the late pseudosteady-state period, ($A=X_{eA}*X_f$, $X_f=100$)

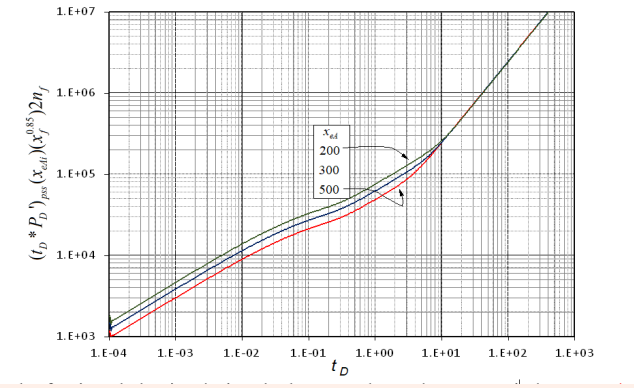

By substituting the dimensionless time from Equation (1) and the dimensionless pressure derivative from Equation (3) into Equation (20) and solving for the SRV area (XeA*Xf), we obtain the following for oil wells:

$$A = 3.7685_{0.87}\sqrt{\frac{q\mu Bt_{pss}}{h(2n_f)(t*\Delta P')_{pss}\phi c_t x_f^2}} \quad (21)$$

Similarly, by substituting Equations (4) and (6) into Equation (20), we obtain the following for gas wells:

$$A = \frac{5848108.15Tq_{sc}}{h(n_f)[t*\Delta m(P)']_{pss}x_f^{0.85}}\sqrt{\frac{t_{pss}}{k_g\phi(\mu c_t)_i}} \quad (22)$$

The point of intersection between the first linear flow regime, Equation (and the late pseudosteady-state period, Equation (20), leads to the following expression:

$$\frac{10.43(t_D^{0.5})_{1lpssi}}{k_o} = \frac{506382(t_D)_{1lpssi}}{(x_{eAi})x_f^{0.85}2n_f} \quad (23)$$

Substitution of the dimensionless time, either Equation (1) or (4) and solving for the SRV area, it is obtained:

$$A = \frac{394.16}{x_f^{0.85}n_f}\sqrt{\frac{k_g^3 t_{1lpssi}}{\phi(\mu c_t)_i}} \quad (24)$$

Equation (24) also applies to oil wells. Both Equations (21) and (22) are affected by the ε value, as shown in Figure 7. Therefore, a correction factor is needed. The different intercepts of the late-time pseudosteady-state straight line are plotted against ε and shown in Figure 8. From this, a correction factor plot is created and provided in Figure 9, leading to the following expression:

$$f_{corr} = 0.7033\varepsilon^5 + 0.9842\varepsilon^4 + 0.4524\varepsilon^3 + 0.7571\varepsilon^2 + 1.2295\varepsilon + 1 \quad (25)$$

$$A_{corr} = \frac{A}{f_{corr}} \quad (26)$$

The developed equations applied to both buildup and drawdown tests.

Figure 7: Pressure derivative vs. time log-log plot for different ε values.

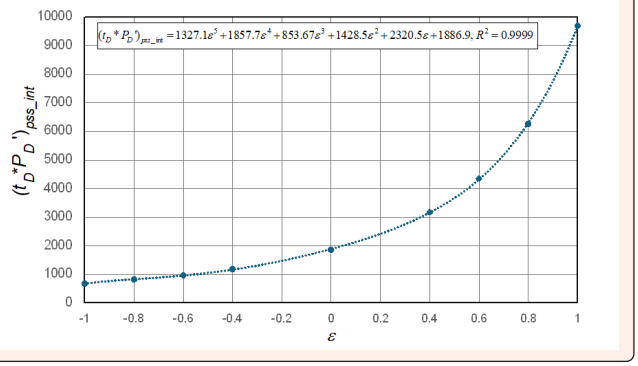

Figure 8: Pseudosteady-state line intercept as a function of ε (pressure transient analysis).

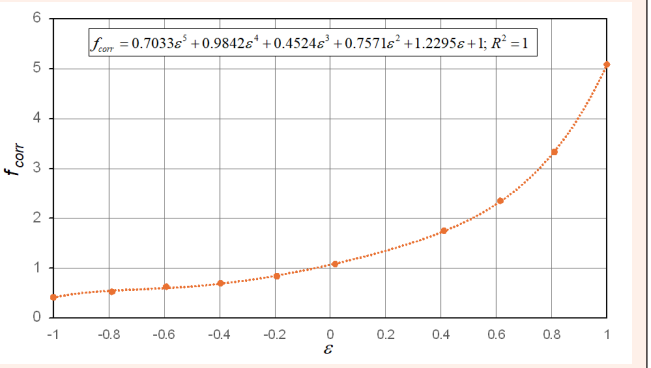

Figure 9: SRV Area correction factor (pressure transient analysis).

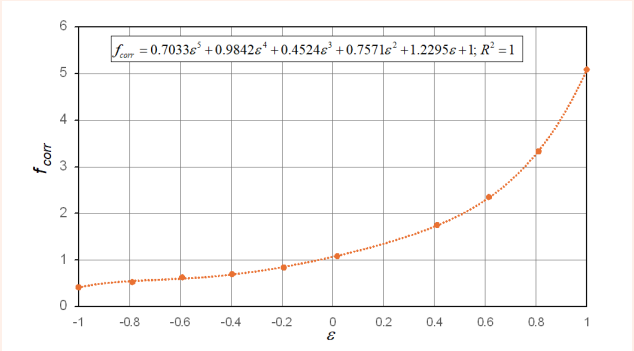

Synthetic Example

Example 1

Next, a synthetic example is solved using the proposed equations. In a shale reservoir field, a hydraulically multi-fractured oil well was drilled. Ten fracturing stages were performed in the well. The well is located between two MFHW wells, B and C, which have been producing for 2 years. The goal is to determine if well A is exhibiting fracture interconnection with wells B and C, and if so, to determine the fraction of interconnected fractures. Below are the data for well A. Pressure derivative versus time data are plotted in Figure 10.

Figure 10: Pressure and pressure derivative log-log plot for the synthetic example 1.

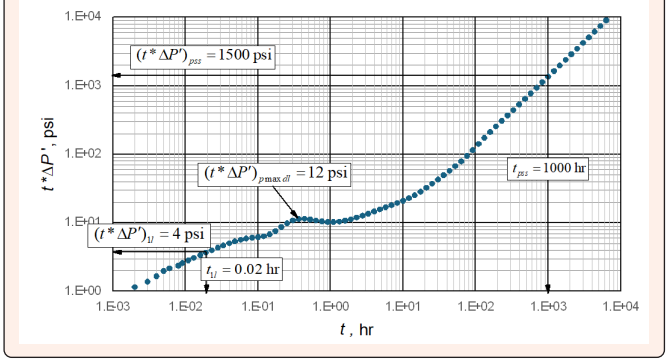

Exercise Data:

$\mu = 0.7$ cp $B_o = 1.35$ rb /STB $c_t = 1x10^{-5}$ 1/psi

$\phi_{SRV} = 15$ % h = 100 ft T = 640 °R

$x_{fA} = 100$ ft $n_f = 10$ $x_{eA} = 300$ ft

$q_A = 350$ BPD $k_o = 10$ md $\varepsilon = 0.62$

A = 22.5 Ac

The following information was read from Figure 5.

$t_{1l} = 0.02$ hr $(t*\Delta P')1l = 4$ psi $(t*\Delta P')pmaxdl = 12$ psi

$t_{pss} = 1000$ hr $t*\Delta P')pss = 1500$ psi

Estimation of k_o and ε with Equation (12) and (15)

$$k_o = 1.5\sqrt{\frac{23.935q\mu^{0.5}B}{h(t*\Delta P')_{1l}}}\sqrt{\frac{t_{1l}}{\phi c_t x_f^2}} = 1.5\sqrt{\frac{23.935(350)(0.7)^{0.5}(1.35)}{(100)4}}\sqrt{\frac{0.02}{(0.15)(0.00001)(100)^2}} = 9.9 \text{ md}$$

Calculation of epsilon: It can be seen in the pressure derivative vs. time graph (Figure 5) that after the first linear flow, there is a downward concavity, indicating a certain degree of fracture interconnection:

$$\varepsilon = 0.18\sqrt{\left(\frac{k_{1A}h(t*\Delta P')_{pmaxdl1l}}{39.201196q\mu B}\right)} = 0.18\sqrt{\left(\frac{9.9(100)(12)}{39.2012(350)(0.7)(1.35)}\right)} = 0.62$$

This indicates that the fraction of fractures in well A that are connected is 0.62 or 62%, meaning that 62% of the fractures in the observation well (Well A) are interconnected with the nearby wells (B-C). The SRV area is found with Equation (21):

$$A = 3.7685\left(0.87\sqrt{\frac{q\mu Bt_{pss}}{(t*\Delta P)_{pss}h(2n_f)\phi c_t x_f^2}}\right)$$

$$A = 3.7685\left(0.85\sqrt{\frac{(350)(0.7)(1.35)(1000)}{(100)(20)(1500)(0.15)(0.00001)(100)^2}}\right) = 51.4 \text{ acres}$$

A correction factor of 2.29 is estimated with Equation (25).

$$f_{corr} = 0.7033(0.62)^5 + 0.9842(0.62)^4 + 0.4524(0.62)^3 + 0.7571(0.62)^2 + 1.2295(0.62) + 1 = 2.29$$

Then, applying the area correction factor, Equation (26), the corrected SRV is estimated:

$$A_{corr} = \frac{A}{f_{corr}} = \frac{51.4}{2.29} = 22.45 \text{ ac}$$

Solution: According to the ε result, the well presents a 62% fracture interconnection with the neighboring wells. The reservoir area calculation confirms the connectivity of well A with the neighboring wells, making it necessary to correct the area. Expressions for reservoir characterization under transient rate analysis conditions are given in Appendix A and B for oil and gas shale reservoirs.

Appendix A: Transient rate analysis equations for oil wells

In a similar way as performed in pressure transient analysis, the governing equation for the early or first linear flow regime is given by:

$$[t_D * (1/q_D')_{1l}]k_o^{1.05} = 1.47\sqrt{(t_D)_{1l}} \quad (A.1)$$

Substitution of Equations (1) and (8) into Equation (A.1) provides:

$$k_o = 11.210\left(\frac{B}{h(\Delta P)[t*(1/q')]_{1l}x_f}\sqrt{\frac{\mu t_{1l}}{\phi c_t}}\right)^{0.6452} \quad (A.2)$$

The governing equation for -1 ≤ ε ≤ 0 is:

$$0.0469 = t_D * (1/q_D')\varepsilon^{0.55} \quad (A.3)$$

Replacing Equation (8) into Equation (A.3), it yields:

$$\varepsilon = 31.1\left(\frac{\mu B}{kh(\Delta P)[t*(1/q')]_{pmindl1l}}\right)^{1.8182} \quad (A.4)$$

The governing equation for 1 ≤ ε ≤ 1 is:

$$0.413 = \frac{t_D * (1/q_D')}{\varepsilon^{0.433}} \quad (A.5)$$

Substituting Equation (8) into Equation (A.5) results in:

$$-\varepsilon = \frac{1}{11968.09}\left(\frac{kh\Delta P[t*(1/q')]_{pmaxdl1l}}{\mu B}\right)^{2.3095} \quad (A.6)$$

The pseudosteady-state period does not exhibit a linear behavior as seen in transient pressure analysis, which typically shows a unit-slope line. Instead, the behavior is asymptotic, and the reciprocal rate and reciprocal rate derivative intersect at a point during the pseudosteady-state period, as shown in Figure A.1. Figure A.2 illustrates the unified behavior for this point, from which:

$$(t_D)_{pss} A^3 = 3.44\times10^{19} \quad (A.7)$$

Figure A.1: Log-log plot of reciprocal rate and reciprocal rate derivative for two values of fracture length and X_{eA} = 5000 ft.

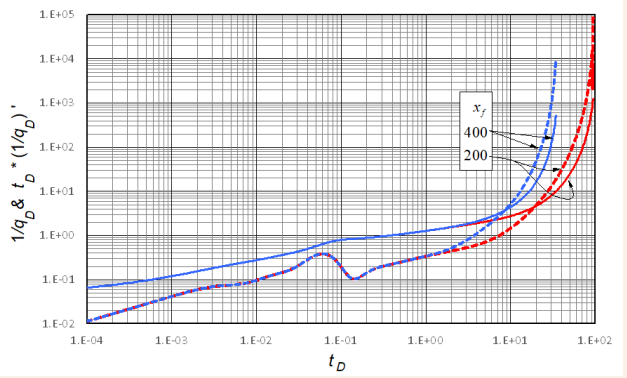

Figure A.2: Unified log-log plot of reciprocal rate and reciprocal rate derivative for two values of SRV area.

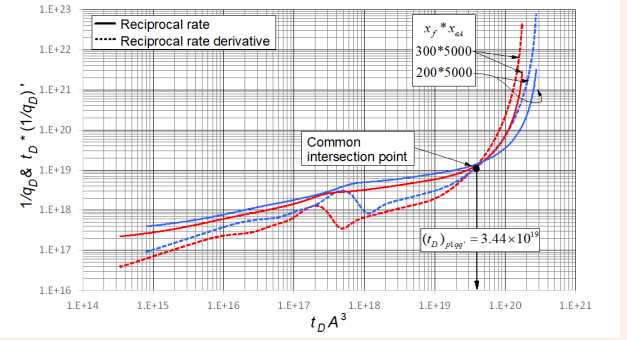

After substituting Equation (1), or Equation (4) for gases, and solving for x_f and multiplying by the wellbore length, L_w, it yields:

$$A = 50716519\sqrt{\frac{\phi\mu c_t x_f^2}{k_o t_{p1qq'}}} \quad (A.8)$$

Appendix B: Transient rate analysis equations for gas wells

Substituting Equation (4) and (8) into Equation (A.1); Equation (4) into Equations (A.3) and (A.5); and Equation (4) into Equation (A.7), we obtain expressions for the estimation of gas permeability, epsilon (ε) and SRV area,

$$k_o = 11.372\left(\frac{T}{h[(\Delta m(P)][t*(1/q')]_{1l} x_f}\sqrt{\frac{t_{1l}}{\phi(\mu c_t)_i}}\right)^{0.6452} \quad (B.1)$$

$$\varepsilon = 2073.882\left(\frac{T}{kh\Delta m(P)[t*(1/q')]_{p\min d1l}}\right)^{1.8182} \quad (B.2)$$

$$-\varepsilon = \frac{1}{2482782.32}\left(\frac{kh\Delta m(P)[t*(1/q')]_{p\max d1l}}{T}\right)^{2.3095} \quad (B.3)$$

$$A = 50716519\sqrt{\frac{\phi(\mu c_t)_i x_f^2}{k_g t_{p1qq'}}} \quad (B.4)$$

The SRV (Stimulated Reservoir Volume) area should be adjusted similarly to transient pressure analysis. It is recommended to plot the intersection points between the reciprocal rate and the reciprocal rate derivative for a given fracture length and various ε values to derive an appropriate equation. In this context, it is assumed that the same correlation factor used in pressure transient analysis applies here. However, instead of using the intercept of the late-time unit slope from the pseudosteady-state period, the intersection point between the reciprocal rate and the reciprocal rate derivative is utilized.

Example 2

Figure 11 contains a log-log plot of pressure derivative versus time for an HMFW oil well with certainty that there is no interconnection with any other well. Notice that this example is similar to example 1 with changes only of the interconnectivity parameter, ε, and the initial pressure. Estimate the SRV area of the observation well. The following data for this example are provided below: Since the characteristic flow regime of fracture interconnection concavity does not form after the first linear flow, and the second linear flow period also does not form, it is most likely that there is no fracture interconnection. In this case, it is advisable to calculate the area with Equation (21) to verify that the SRV area is similar to the area with which the HMWF well was designed. Solution: Since this well does not present fracture interconnection with any other well, the area value does not need to be corrected. Therefore, the area of this well is similar to the design area of the HMFW well, A = 22.5 acres. Discussion

Figure 11: Pressure and pressure derivative log-log plot for the synthetic example 2.

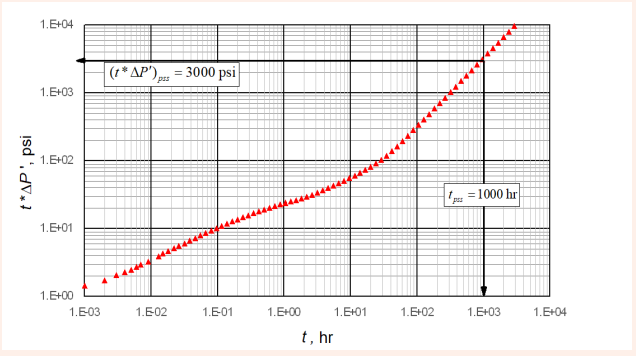

Discussion

The generated equations were successfully applied to the pressure derivative versus time data, approximately reproducing the permeability, epsilon (ε), and area data, which are functions of the original design area of the HMWF in case of interconnected fractures. It was observed that when there is fracture interconnection, an upward or downward concavity is evident. The maximum or minimum point of this concavity in the pressure derivative versus time is crucial for determining the degree of fracture interconnection that Well A has with the neighboring wells, which is the objective of this work.

Conclusion

a. Direct analytical equations were developed to determine the degree of fracture interconnection in a system of three horizontal wells in a shale reservoir. The generated equations were successfully verified using synthetic problems, demonstrating their accuracy and usefulness.

b. These equations also allow for the estimation of the permeability of the observation well and its drainage area. They can be used in pressure drawdown and buildup tests, as well as in transient rate analysis for both oil and gas wells.

c. The existence of fracture interconnection causes an increase or decrease in the drainage area of the observation well.

d. This degree of interconnection is estimated using the maximum or minimum value of the concavity observed in the pressure derivative after the first linear flow regime.

e. A correction factor was developed to estimate the degree of deviation of the real area concerning the drainage area affected by the influx or flow of the SRV from Well A to the nearby wells. This correction factor varies between 0.6% and 400%, depending on the value of epsilon (ε).

References

1. Jacobs T (2017a) Frac hits reveal well spacing may be too tight, completion volumes too large. Journal of Petroleum Technology 69(11): 35-38.
2. Lawal H, Jackson G, Abolo N, Flores C (2013) A Novel approach to modeling and forecasting frac hits in shale gas wells. Paper presented at the EAGE Annual Conference & Exhibition incorporating SPE Europec, London, UK.
3. Jia P, Cheng L, Clarkson CR, Qanbari F, Huang S, et al. (2017) A laplace-domain hybrid model for representing flow behavior of multifractured horizontal wells communicating through secondary fractures in unconventional reservoirs. SPE Journal 22: 1856-1876.
4. Frohne KH, James CM (1984) Fractured shale gas reservoir performance study-an offset well interference field test. Journal of Petroleum Technology 36(2): 291-300.
5. Hetrick LH (2019) Frac Hit: Well-to-well communication.
6. Jacobs T (2017b) Oil and gas producers find frac hits in shale wells a major challenge. Journal of Petroleum Technology 69(4): 29-34.
7. Yu W, Wu K, Zuo L, Tan X, Ruud W (2016) Physical models for inter-well interference in shale reservoirs: Relative impacts of fracture hits and matrix permeability. Paper presented at the SPE/AAPG/SEG Unconventional Resources Technology Conference, San Antonio, Texas, USA.
8. Molina OM, Zeidouni M (2017a) Analytical approach to determine the degree of interference between multi-fractured horizontal wells. Paper presented at the SPE Europec featured at 79th EAGE Conference and Exhibition, Paris, France.
9. Molina OM, Zeidouni M (2017b) Analytical model to estimate the fraction of fracture hits in a multi-well pad. Paper presented at the SPE Liquids-Rich Basins Conference - North America, Midland, Texas, USA.
10. Molina OM (2019) Analytical model to estimate the fraction of frac hits in multi-well pads. Paper presented at the SPE/AAPG/SEG Unconventional Resources Technology Conference, Denver, Colorado, USA.
11. Tiab D (1995) Analysis of pressure and pressure derivative without type-curve matching-skin and wellbore storage. Journal of Petroleum Science and Engineering 12(3): 171-181.
12. Bernal KM, Escobar FH, Ghisays-Ruiz A (2014) Pressure and pressure derivative analysis for hydraulically fractured shale formations using the concept of induced permeability field. Journal of Engineering and Applied Sciences. 9(10): 1952-1958.
13. Escobar FH, Bernal KM, Olaya-Marin G (2014) Pressure and pressure derivative analysis for fractured horizontal wells in unconventional shale reservoirs using dual-porosity models in the stimulated reservoir volume. Journal of Engineering and Applied Sciences 9(12): 2650-2669.
14. Escobar FH, Rojas JD, Ghisays-Ruiz A (2015) Transient-rate analysis for hydraulically fractured horizontal wells in naturally fractured shale gas reservoirs. Journal of Engineering and Applied Sciences 10(1): 102-114.
15. Escobar FH, Cabrera MA, Ortiz AJ (2018) Pressure derivative analysis for horizontal wells in shale reservoirs under trilinear flow conditions. Journal of Engineering and Applied Sciences 13(10): 3426-3434.
16. Escobar FH, Prada EF, Suescún-Diaz D (2021) Interpretation of pressure interference tests for wells connected by a large hydraulic fracture. Journal of Petroleum Exploration and Production Technology 11: 3277-3288.
17. Gomez-Gil DF, Sacanabuy AD (2023) Estimation of the fraction of interconnected fractures in a model of three horizontal wells in source rock reservoirs through analysis of pressures and transient flows (Degree Thesis). Surcolombiana University, Neiva, Huila, Colombia.